Determination of the water content of fillerised fine aggregates in the saturated surface dry state

Patrick Gentilini, Oumaya Yazoghli-Marzouk, Vincent Delmotte, Yannick Descantes

GENTILINI, Patrick, YAZOGHLI-MARZOUK, Oumaya, DELMOTTE, Vincent, DESCANTES, Yannick, 2015, Determination of the water content of fillerised fine aggregates in the saturated surface dry state, Construction and Building Materials, 98, Elsevier, pp.662-670, DOI: 10.1016/j.conbuildmat.2015.08.131

Determination of the water content of fillerised fine aggregates in the saturated surface dry state

P. Gentilini, O. Yazoghli-Marzouk, V. Delmotte, Y. Descantes[1]

Abstract

An experimental setup designed to capture the saturated surface dry (SSD) state of porous fine aggregates incorporating significant amounts of fines is presented. This setup is validated upon testing fine aggregate sources with different water absorption values up to 5.6 %, and at least 8 % of fines. Test duration is found to lie in the 120-to-240-minute-range, depending on test sample initial mass and water content. Several procedures for calculating the water content in SSD state are presented and discussed. One of these procedures uses the drying theory to fit curves depicting water content shift as a function of drying time and identify breakpoints. A more straightforward strategy is focused on the transition point between retained and free water on charts representing the variations of water content as a function of relative humidity. In both cases, fairly repeatable and discriminant water content values in SSD state are obtained. As expected, these values are found significantly higher than those determined in the absence of fines according to the usual cone test [1]. Moreover the lack of reliability of water absorption values determined in the presence of fines according to the cone test procedure is verified. Eventually, several perspectives are pointed out to improve the setup which could easily be automated.

Keywords: fine aggregate, sand, cement concrete, water absorption, test method, experimental setup, drying

[1] Corresponding author, yannick.descantes@ifsttar.fr

1. Introduction

Short term and long term performances of cement concrete are known to depend on effective-water-to-cement ratio (W_{eff}/C), where effective water refers to water available for cement hydration. Effective water may be defined as the total mass of water contained in the cement concrete (W_{tot}) less the mass of water retained by the aggregate fractions. For a given aggregate source, this 'retained water' is known to increase with decreasing size fraction, especially in the fine fractions 0/4 or 0/5 mm. The maximum retained water is routinely though disputably [2] assessed by the 'water absorption' value (WA) – mass of water penetrating the voids of particles during a prescribed period of time, routinely 24h, expressed as a percentage of the oven-dried mass of the aggregate sample [1]. For a long time, the large quantities of fine aggregates needed for cement concrete production have been purveyed almost exclusively by natural fine aggregates (NFA) from alluvial or limestone deposits, whose WA values are known to be low (< 1%). In the recent years, the shortage of alluvial sources and waste storage capacity limitations have given rise to a worldwide interest in abundant alternative fine aggregate sources such as recycled concrete fine aggregates (RCFA). However, their use is still limited due to high WA values in the range 6-10 % [3,4].

Indeed, adjusting the W_{eff}/C ratio of fresh cement concrete becomes much more difficult when fine aggregates with high WA value are incorporated, since they may add or subtract water allotted for cement hydration, thus impact its short term workability as well as mechanical and durability performances in hardened state [5][6]. Khatib [7] reported the good workability of fresh cement concrete incorporating 100% RCFA with additional water to reach W_{tot}/C = 0.5 (no plasticizer); however, he also noted a compressive strength drop down to 35% after 28 days of curing and a drying shrinkage

47 increase up to 50% when compared with a reference cement concrete incorporating
48 NFA exclusively. Reducing the W_{tot}/C ratio upon using an admixture allows both to
49 maintain sufficient workability and prevent compressive strength drop, but concrete
50 properties in hardened state are still impacted: splitting resistance may decrease by
51 30%, water absorption and sorptivity may increase by 46% and 70% respectively with
52 respect to corresponding values of the reference cement concrete. As a consequence,
53 external fluids may penetrate the concrete microstructure and introduce deleterious
54 substances such as carbon dioxide and chloride ions, causing concrete carbonation and
55 steel corrosion respectively [8].

56 The water absorption of alternative fine aggregates such as RCFA having
57 significant implication on W/C ratios for concrete mixtures, determining it accurately is
58 critical [4]. Therefore, most test methods consist of drying a pre-saturated sample until
59 achievement of the state under which particles surface is free of vaporizable moisture
60 but their accessible pores remain saturated with water, called saturated-surface-dry
61 state (SSD, see Figure 1), then in promptly weighing the sample. To capture the SSD
62 state, some methods focus on the visual detection of test portion color change when
63 particles become free of surface vaporizable moisture [9,10]. Others track the slump of
64 a cone-shaped test portion [1,11,12] or the flow of a test sample off a tilted masonry
65 trowel [10] which occur when between-particles surface tension forces disappear.
66 Others spot slope breakpoints on curves measuring physical characteristics of test
67
68
69

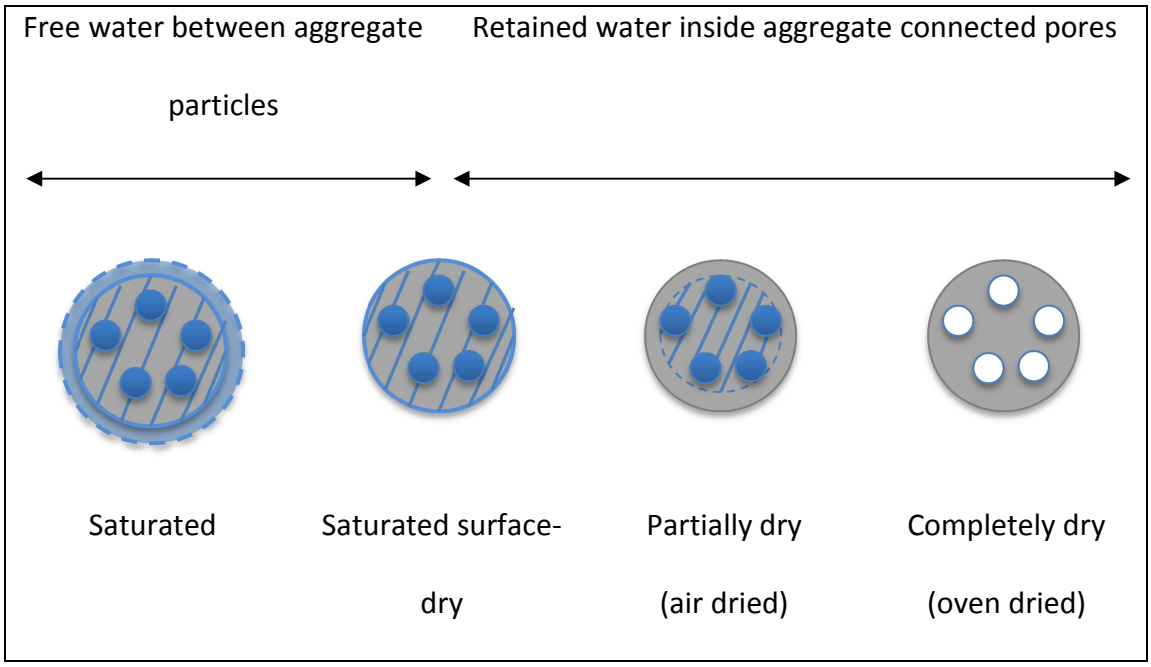

Fig. 1. Schematic view of an aggregate particle for various water content values.

samples as a function of drying time, such as electrical resistivity reflecting the presence of between-particles water bridges [13]. A few test methods attempt to detect the end of the saturation phase while soaking a dry test portion, either from direct measurement of the volume of absorbed water [14], or from detecting the reflection signal of infra-red light rays when particles surface becomes moist [15]. Unfortunately, most of these test methods are unsuitable for fine aggregates such as RCFA, which may incorporate up to 10-13% of fines (particles passing the 0.063 mm sieve) [16,17]. Indeed, Rogers et al [18] have reported a 100% overestimation of WA values assessed from methods using the cone slump criterion [1,11,12], which they allotted to fines adhering to larger particles and forming clusters, thus trapping part of the formerly free water into their inner structure and causing earlier achievement of the sample 'SSD' state than in the absence of fines. Similarly, methods focused on test portion color change yield scattered results in the presence of fines, since homogenously drying a sample becomes delicate [19].

Promising WA values of fine aggregates were measured using test methods derived from thermodynamic [19,20] or industrial drying approaches [21]. The former consists in air drying a pre-saturated fine aggregate sample placed into a rotating drum closed at both ends by 0.075 mm square mesh screens, while recording the temperature gradient between drum inlet and outlet as well as relative humidity at drum outlet. The drying phase is stopped and the sample is weighed when the temperature gradient or relative humidity curves evidence breakpoints similar to those shown on Fig. 2, presumably representative of SSD state according to the authors. The latter assimilates the drying of soaked aggregates at rest in a chamber to the evaporation of water from a porous medium at constant air temperature. Fig. 3 depicts sample mass reduction through evaporation as a function of time, which consists of three well-known phases [22]:

- a transition phase corresponding to the drying chamber conditioning;
- then, a linear part depicting the evaporation of surface water at a constant rate monitored by environmental conditions (temperature and relative humidity) until achievement of the SSD state;
- Eventually, a phase at decreasing mass reduction rate evidencing the evaporation of absorbed water from aggregate pores.

Though promising, these two test methods have drawbacks: the drum method is biased by a loss of fines through the screens and disassembly operations which delay the weighing once SSD state is achieved; the drying chamber is unsuitable for uniformly drying polydisperse fine aggregates at rest due to crusting effects [22].

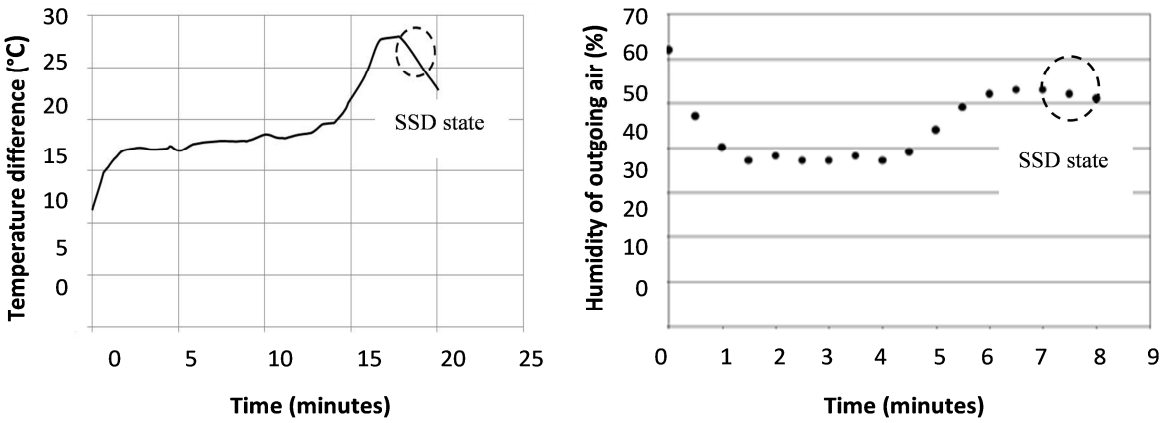

Fig. 2. Temperature gradient versus time (left) and relative humidity versus time (right) plots [19].

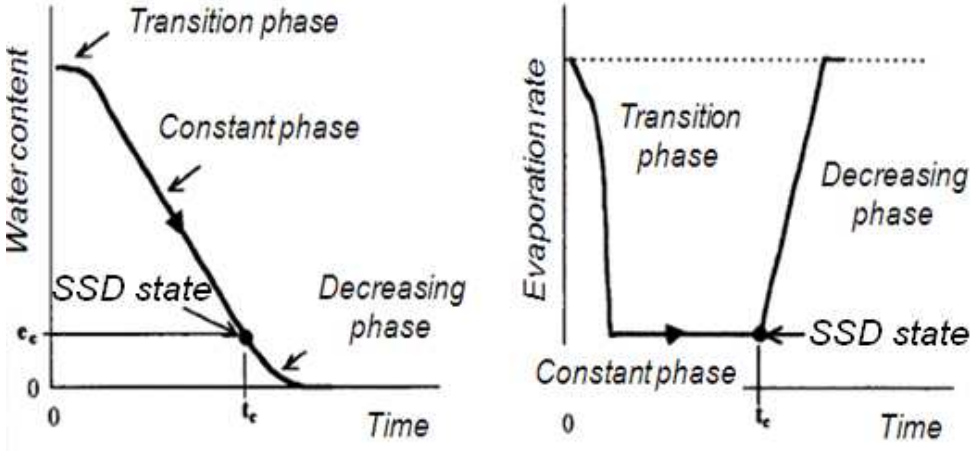

Fig. 3. Water content (left) and evaporation rate (right) in a porous material [21].

In order to determine the water absorption of fine aggregates incorporating fines, the present paper introduces an improved experimental setup designed to capture the SSD state and measure the water content in this state. Section 2 describes the experimental setup and the test program designed for its validation. Section 3 investigates the presence of breakpoints on various curves representing recorded data and discusses methods for assessing the water content in SSD state.

2. Experimental setup and test program

a. Experimental setup

The experimental setup used to capture the SSD state is inspired from early development by Dana et al [20] and subsequent development by Kandhal et al [19]. As shown in Fig. 4, it is composed of a hair dryer that blows warm air at one end of a rotating drum, which is mounted on caster wheels and driven by a belt through a step motor. The drum incorporates flights to stir the test sample in order to achieve reasonably uniform drying, as well as screens at drum inlet (0.063 mm opening) and outlet to reduce aggregates loss. Temperature is measured by two probes located at either ends of the drum and relative humidity is captured by a hygrometry probe located at drum outlet. However, three major improvements have been implemented: first, both the screen blinding and loss of fines issues reported by Kandhal et al [19] have been sorted out using respectively an outlet screen with a wider opening (0.5 mm), and a fines collector consisting of a simple vortex system equipped with a cup, in which fines will remain trapped till the end of the test (see Fig. 4); second, no more drum removal is needed for weighing as the full experimental setup is mounted on a balance, thus allowing continuous weight monitoring to ± 1 g; third, the air dryer is fed by a voltage regulator to monitor the blown air temperature to roughly 70°C, that is not too high to avoid removing crystallized water in the mortar attached to the aggregate [23,24] though sufficiently high to keep the drying time reasonable. The total mass of unloaded experimental setup mounted on the balance is 13.1 kg.

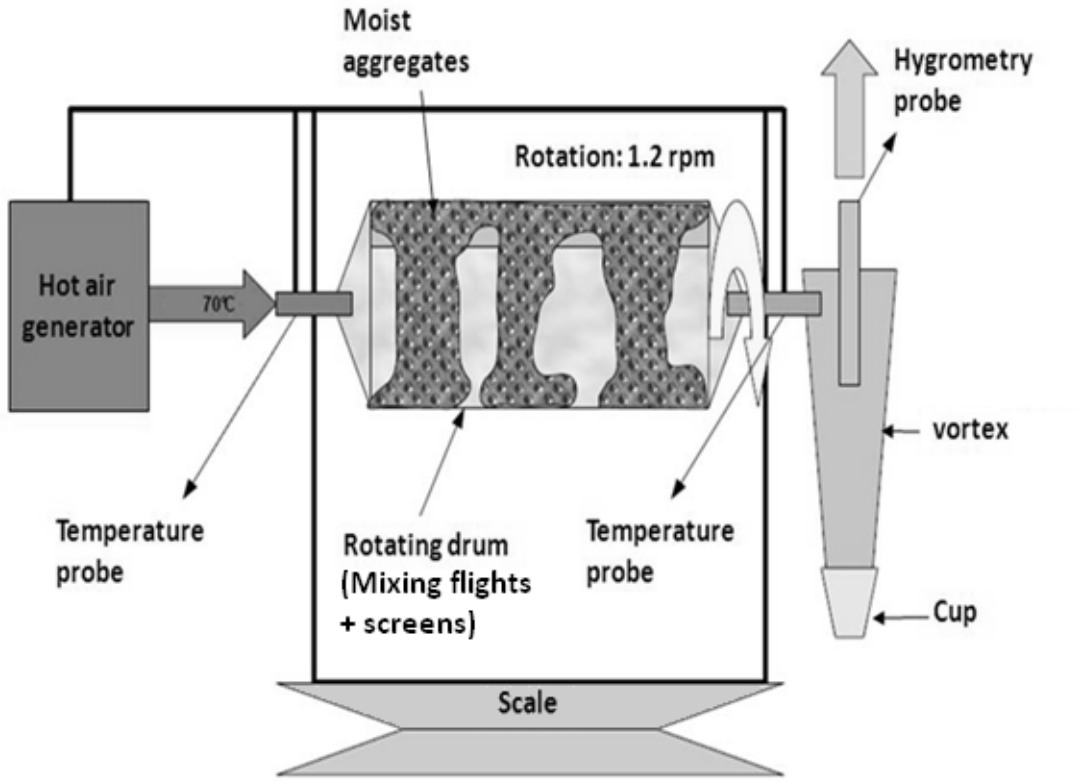

Fig. 4. The experimental set-up used for the determination of SSD state.

b. Test program

Tested materials were sampled from three different sources, crushed sand-lime alluvium, crushed limestone and recycled concrete. Fig. 5 depicts the mean grading curve of each material tested, all of them incorporating at least 8% fines. Table 1 summarizes the densities and water absorption values determined for each material according to EN 1097-6 clause 9. The selected materials cover a reasonably wide range of WA values, from 0.8 for NFA up to 5.6% for RCFA, and the corresponding densities vary conversely as already noticed elsewhere [7,25]. Although the test procedure depicted in EN 1097-6 clause 9 prescribes fines discarding, a second set of samples were tested with their fines, supplemented with methylene blue (MB) tests

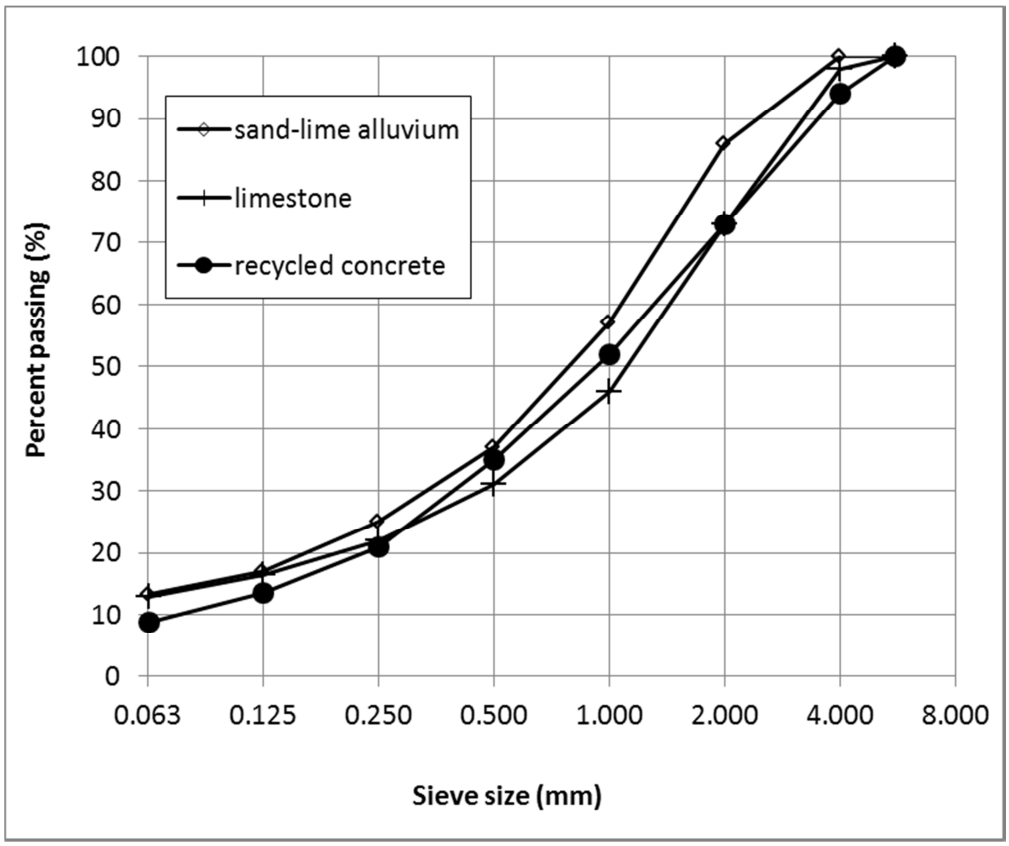

Fig. 5. Grading curves of tested materials.

Table 1. Densities, water absorption and MB values of tested sands.

		sand-lime alluvium		limestone	recycled concrete	
		#1	#2		#1	#2
immersion time (h)		24		24	96	
no fines	**ρ_{ssd} (t/m^3)**	2.68	2.67	2.61	2.41	-
	WA_{24} (%)	0.8	1.1	2.2	5.6	-
with fines	**WA_{24} (%)**	1.5	-	5.4	7.1	7.3
	ρ_{ssd} (t/m^3)	2.65	-	2.50	2.34	2.36
	MB (g/kg)	0.8	-	0.9	-	-

166 performed on 0/2 mm samples in accordance with EN 933-9 [26] to check the fines
167 quality. As expected [18], water absorption values in the presence of fines are
168 systematically higher than those measured without fines, although MB values suggest
169 low clay contents.

170 For each material source, three 0/4 mm test samples were prepared with
171 random dry masses and initial moisture contents as mentioned in Table 2. Moisture
172 content differences were obtained upon immersing each sample for at least 24h (96 h
173 for RCFA, see Table 1) and then letting it drain at room temperature for some time.
174 Samples were subsequently introduced into the experimental setup and air dried until
175 their masses reach equilibrium. Meanwhile, room, drum inlet and outlet temperatures
176 were recorded every second, as well as relative humidity. Every minute, the drum
177 rotation was stopped for a few seconds in order to record the mass of the loaded
178 experimental setup. Once the mass equilibrium was achieved, each sample was further
179 oven-dried at 105°C until constant mass in order to assess its dry mass according to EN
180 1097-5.

181 Table 2. Dry masses and initial moisture contents of the test samples.

	sand-lime alluvium			**Limestone**			**recycled concrete**		
	#1	#2	#3	#1	#2	#3	#1	#2	#3
Immersion time (h)	24			24			96		
Dry mass (g)	444.1	940.2	430.8	422.0	590.8	909.8	618.4	408.4	371.6
Initial moisture content (%)	20.0	16.6	18.6	21.2	20.3	18.7	16.1	39.3	39.7

182

3. Results and discussion

a. Water content as a function of drying time

Fig. 6 represents the variations of the water content of all tested samples as a function of drying time. Several observations arise from this figure.

First, the test duration is comprised between 120 and 240 min, which seems much longer than the test duration reported by Kandhal et al [19] with 500-g-samples. However, no objective comparison may be conducted since Kandhal et al [19] discarded particles below 0.6 mm and provided no information on initial water content (the lower the quicker the test) or inlet air temperature (the higher the quicker the test).

Next, the residual water content at the end of the non-linear phase is zero except for RCFA, whose residual water content ranges between 1.4 and 1.9 %. This observation suggests that, as expected, the moderate drying temperature used (70°C) efficiently prevents the dehydration of hydrates, with part of the water remaining trapped into micropores or mesopores of the cement paste [27–29]. This aspect will not be investigated further as it falls beyond the scope of the present paper.

Furthermore, despite the absence of a transition phase that may be explained by a rather low thermal inertia of the experimental setup, any curve in Fig. 6 evidences a linear phase depicting the evaporation of surface water at constant rate. This phase is followed by a non-linear one at decreasing evaporation rate, which corresponds to the evaporation of absorbed water. These similarities with the drying theory suggest using it in order to assess the SSD state separating these two phases.

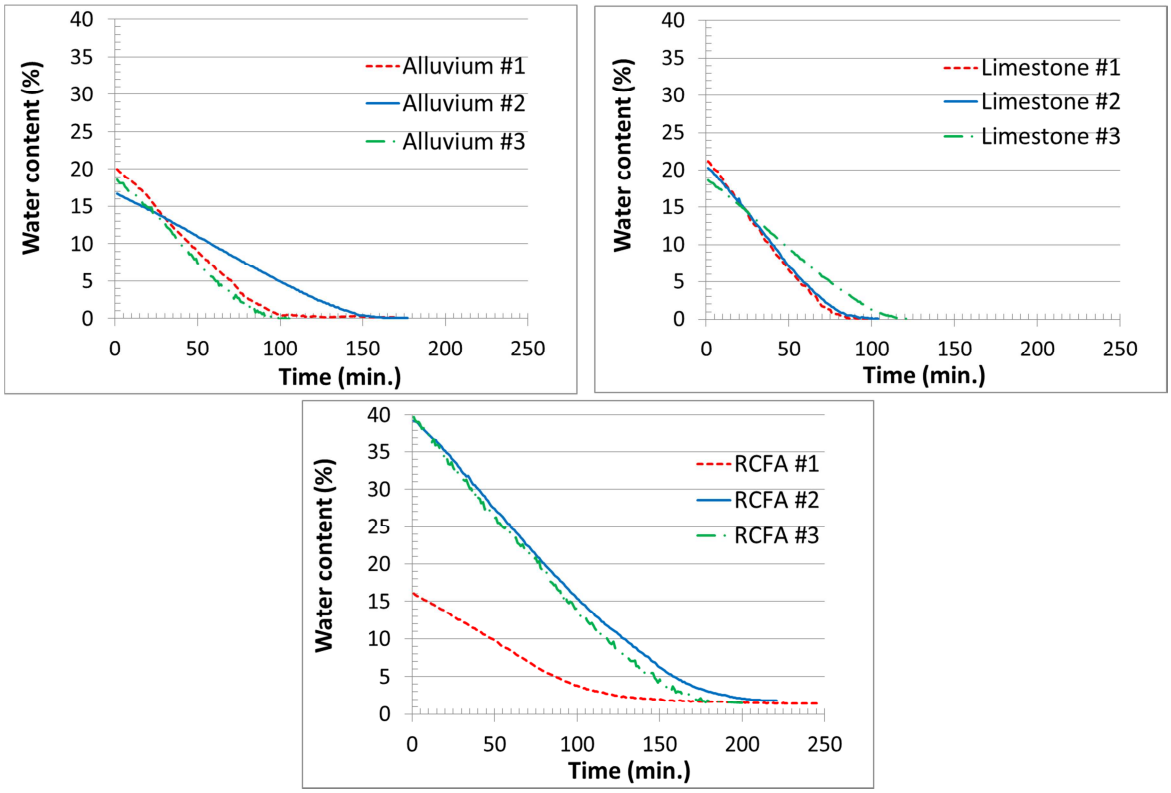

Fig. 6. Water content as a function of time for all tested samples.

b. SSD assessment from water content versus drying time curves

Given the experimental setup used to dry a test sample, assessing its SSD state from the water content versus time curve according to the drying theory principles requires the following three assumptions be made: first, the stirring action of flights inside the rotating drum ensures fairly homogenous drying; second, as long as free water (i.e. not retained by the aggregate) may evaporate, the air/aggregate exchange surface has a constant area that remains saturated; last, variations of the laboratory temperature, relative humidity and air generator temperature are neglected.

Under these assumptions, the evaporation rate during the linear drying velocity phase is controlled exclusively by the air/aggregate exchange surface area and the

thermodynamic characteristics of the humid air inside the rotating drum (relative humidity and temperature). Hence it may be expressed as [22]:

$$\frac{dW}{dt} = -\frac{hA(T_a - T_s)}{L_v M_s} = -\frac{ha(T_a - T_s)}{L_v \rho_{app}} = -C_1 \qquad \text{for } W \geq W_{SSD} \qquad (1)$$

where W is the test sample water content (%), h is the thermal transfer coefficient between air and test sample surface ($W.m^{-2}.K^{-1}$), A is the air/test sample exchange surface area (m^2), T_a - T_s is the mean difference between air and test sample surface temperatures inside the rotating drum (in K, T_s being equal to the air humid temperature), L_v is the latent heat of vaporization at test sample surface temperature ($J.kg^{-1}$), M_s is the test sample dry mass (kg), a and ρ_{app} are the specific surface (m^2/m^3) and apparent density (kg/m^3) of the test sample respectively, and C_1 is a positive constant ($\%.s^{-1}$). Observe from equation (1) that the slope of this linear phase shall be material dependent, since different materials generally have different grading curves, hence different specific surfaces, and apparent densities. Furthermore, for a given material source, samples with significantly higher masses shall yield significantly lower absolute slopes, since A/M_s ratio in a cylinder decreases when M_s increases (this property, valid as long as the test sample fills no more than half of the rotating drum, may be mathematically demonstrated upon observing that A may be approximated by the horizontal free surface area of the test sample at rest in the same cylinder without flights). Notice that curves depicted in Fig. 6 meet these qualitative predictions.

Still under the same assumptions, the capillary theory applicable to granular test samples allows to express the evaporation rate during the non-linear drying velocity phase as [22]:

$$\frac{dW}{dt} = -C_2(W - W_{res}) \qquad \text{for } W \leq W_{SSD} \qquad (2)$$

where C_2 is a positive constant (s^{-1}) and W_{res} stands for the residual water content of test sample at the end of the drying operation.

Upon integration, equations (1) and (2) yield the following system of equations:

$$\begin{cases} W = -C_1 t + W_0 & for\ t \leq t_{SSD} \\ W = e^{-C_2 t + C_3} + W_{res} & for\ t \geq t_{SSD} \end{cases} \quad (3)$$

Where W_0 is the water content at t=0 according to the linear fit, t_{SSD} is the drying time when $W = W_{SSD}$ and C_3 is a constant. For each curve depicted on Fig.6, constants C_1, W_0, C_2 and C_3 may easily be determined upon fitting the relations of system 3 to their respective phases using the least squares method. Eventually, W_{SSD} may be calculated upon eliminating the time in system (3) at $t = t_{SSD}$ and solving the following equation (for example using the Newton-Raphson's method):

$$f(W_{SSD}) = W_{SSD} - \left(e^{-\frac{C_2}{C_1}(W_0 - W_{SSD}) + C_3} + W_{res}\right) = 0 \quad (4)$$

For each curve depicted on Fig. 6, Table 3 summarizes the calculated values of constants C_1, W_0, C_2 and C_3 as well as two coefficients of determination R^2 reflecting the quality of linear and non-linear fits. With R^2 values of 1.00, the linear fits quality is excellent, and the non-linear fits are also very good with R^2 values ranging from 0.84 up to 0.99. A consequence of the capillary theory applied to the drying of fine aggregates is that the rate of evaporation should vary continuously between the linear and non-linear phases. This may be checked upon equalizing equations (1) and (2) when $W=W_{SSD}$ [22], which yields the following relation:

$$C_1 = C_2(W_{SSD} - W_{res}) \quad (5)$$

For each tested sample, Table 3 displays the values of

Table 3. Fit of linear and non-linear phases of drying curves and water content values.

	sand-lime alluvium			**limestone**			**recycled concrete**		
	#1	#2	#3	#1	#2	#3	#1	#2	#3
C_1 (%.min^{-1})	0.227	0.121	0.249	0.306	0.282	0.192	0.133	0.247	0.252
W_0 (%)	20.4	17.1	20.0	21.7	21.4	19.2	16.3	39.9	39.1
R²	**1.00**	**1.00**	**1.00**	**1.00**	**1.00**	**1.00**	**1.00**	**1.00**	**1.00**
C_2	0.069	0.054	0.084	0.085	0.095	0.074	0.030	0.041	0.039
C_3	6.3	7.3	6.8	6.3	7.3	7.3	3.9	7.1	6.6
R²	**0.98**	**0.94**	**0.84**	**0.94**	**0.92**	**0.87**	**0.99**	**0.85**	**0.91**
$\lvert[C_1-C_2(W-W_{res})]/C_1\rvert$	15%	2%	16%	11%	19%	15%	15%	15%	20%
W_{res} (%)	0.1	0.1	0.0	0.0	0.1	0.1	1.4	1.9	1.5
W_{SSD} (%)	2.9	2.3	2.5	3.2	2.5	2.3	6.5	7.0	6.7
W_{trans} (%)	2.7	2.2	2.7	3.5	2.7	2.8	6.4	7.0	6.0
$\lvert W_{trans} - W_{SSD}\rvert$ (%)	0.2	0.1	0.2	0.3	0.2	0.5	0.1	0.0	0.7

$|C_1 - C_2(W_{SSD} - W_{res})|/C_1$ which range between 2 and 20%. These low deviations to zero might reflect minor diffusion phenomena, whose study falls beyond the scope of the present paper.

Table 3 also gathers water content values calculated for each test sample from equation (4). Mean water content values in SSD state for sand-lime alluvium, limestone and RCFA are 2.6, 2.7 and 6.7 % respectively. As expected, observe that these values are higher than corresponding WA_{24} values reported in Table 1 in the absence of fines. With fines, comparison between W_{SSD} and WA_{24} values is chancy, which reflects the irrelevance of the cone slump test in the presence of fines. For any material source but limestone, the standard deviation of W_{SSD} values is about 0.3 %, which is close to the 0.2

% repeatability standard deviation determined on natural fine aggregates in the absence of fines (see EN 1097-6, Table I.4). For limestone, the standard deviation is just below 0.5 due to the relatively high value calculated for test sample #1.

c. SSD assessment from temperature or relative humidity versus time curves

Dana et al and Kandhal et al [19,20] have suggested that the SSD state could be captured upon detecting breakpoints on curves depicting temperature gradient ('inlet – outlet' temperature) or relative humidity as a function of time. In order to check this statement, Fig. 7 represents for each material source tested (one test sample per material) temperature gradient and relative humidity variations as a function of time. Depending on test sample initial mass and water content, as well as heat generator fluctuations (±1.5 °C), these curves acquired every second while both the heat generator and rotating drum were operating appear more or less noisy. To mitigate the noise, mobile means over 60 s (corresponding to the weighing period) have been represented on each chart. These curves are clearly very different from those reported by Kandhal et al [19] (see Fig. 2). Despite a slight downward trend visible mainly on relative humidity curves, the temperature gradient curves and, above all, the relative humidity curves evidence fairly clear drop breakpoints. These are located on each curve past the vertical dotted line depicting the achievement of the *SSD* state as calculated from the corresponding water content versus drying time curves. The temperature gradient drop is caused by test samples warming once free surface water has totally evaporated. However, temperature charts on Fig. 7 show that this warming is

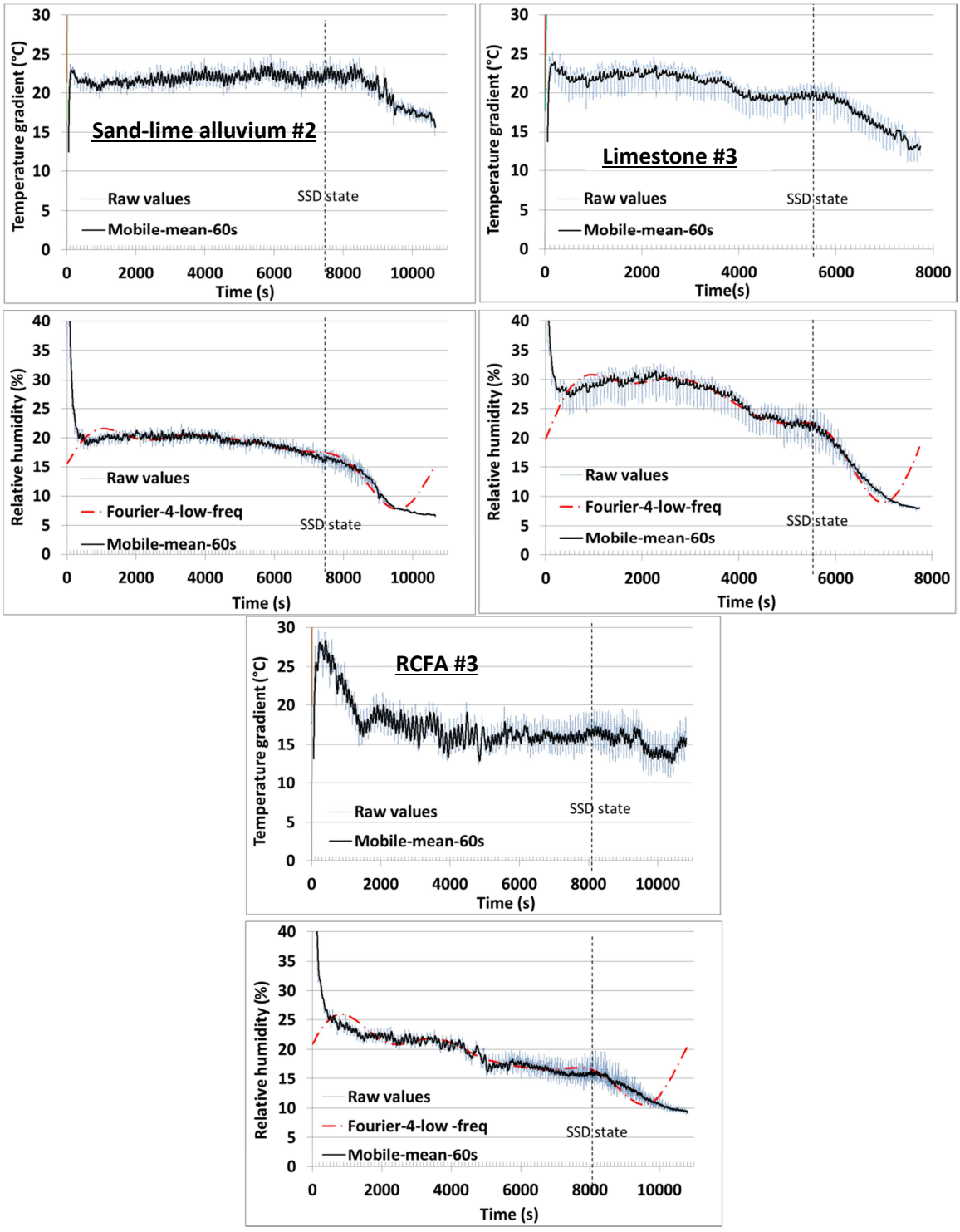

297

298 Fig. 7. Temperature gradient (top figures) and relative humidity (bottom figures)

299 variations as a function of time for all materials tested.

300

offset by 5-25 min. from the *SSD* state, which may be explained by the presence of water trapped in fines porosity and the fairly high specific heat of aggregates (about 1000 $J.Kg^{-1}.K^{-1}$). Contrariwise, Fig. 7 suggests that drop on relative humidity curves occurs more promptly once the *SSD* state is achieved, which tends to confirm the assumption of homogenous drying. Upon sampling every 60s and preserving only the 4 lowest frequencies, Fourier fits performed on relative humidity versus time curves yield smooth curves whose last local maxima just before the drops superimpose remarkably well with corresponding *SSD* states.

d. SSD assessment from water content versus relative humidity curves

In order to improve the straightforwardness and possibly the accuracy of *SSD* state assessment, the two physical properties found to yield the most accurate assessment of the *SSD* state among those recorded were represented one as a function of the other. Hence, for each material tested, Fig. 8 depicts water content variations as a function of relative humidity. Although the inlet temperature is kept reasonably constant all through the drying operations, with the temperature gradient fairly constant until achievement of the *SSD* state (see Fig. 7), curves depicted on Fig. 8 should not be confused with actual water vapour desorption isotherms as defined by IUPAC [30]. Indeed, actual water vapour desorption isotherms are usually determined for a discrete set of relative humidity values, which are successively imposed during several days using various saturated salt solutions until test sample mass achieves an equilibrium [31]. Here, drying operations are quick (less than 4 hours), which partly explains curves fluctuations, and no static equilibrium

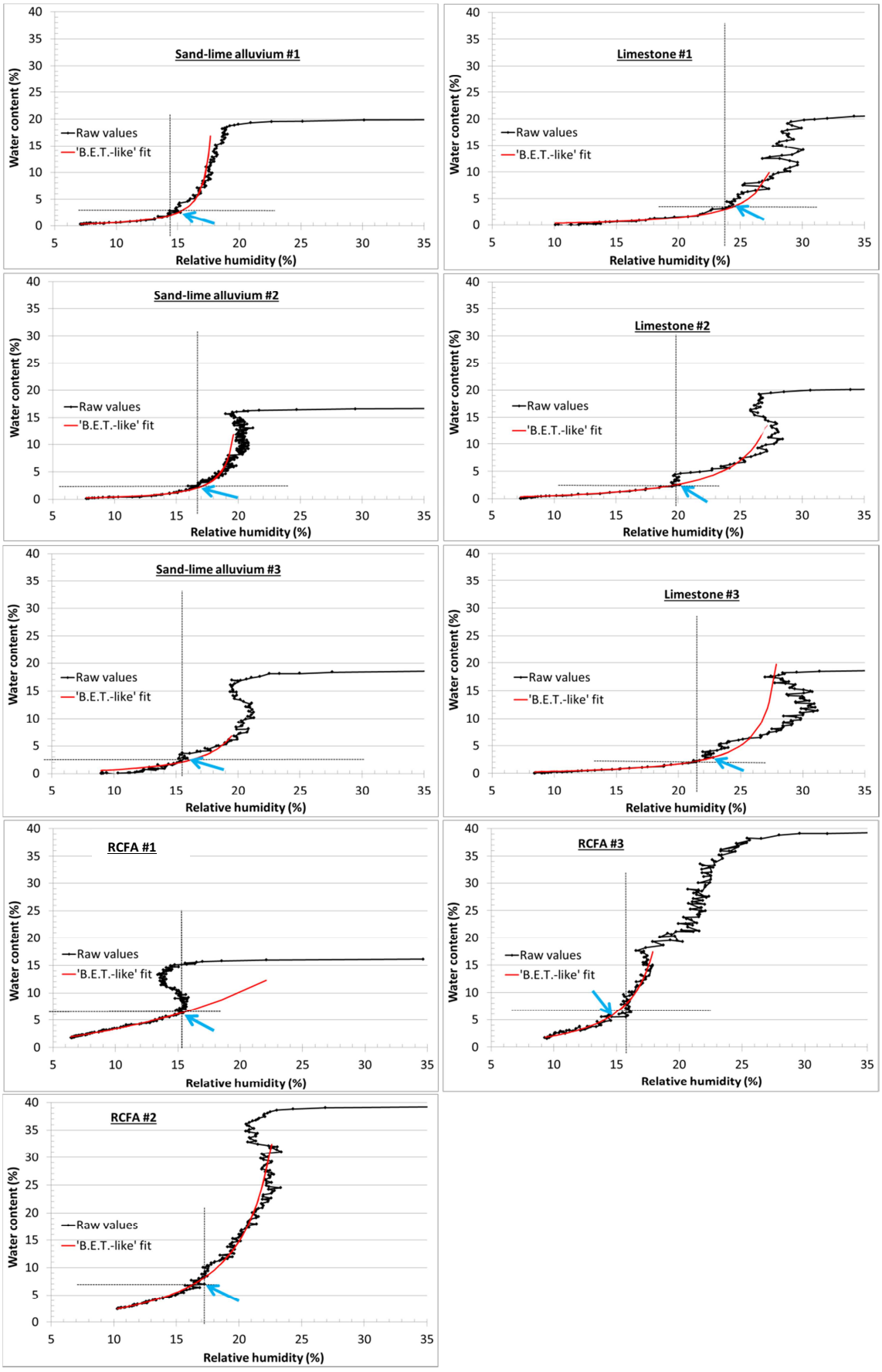

Fig. 8. Water content as a function of relative humidity (3 test samples/material).

state is reached. Nevertheless, the outline of curves depicted in Fig. 8 looks similar to that of water vapour desorption isotherms: a fairly flat phase at the end of the drying operation (relative humidity about 10-15%) corresponds to minor water content shift; this phase is preceded by a steep one evidencing important water content change at higher relative humidity (typically about 15 to 25% depending on material tested). The transition between these two phases may well be seen as the drying point beyond which water becomes much harder to eliminate from the material. In other words, this point is representative of the retained water content assessed by the SSD state. In order to precisely locate this transition point on each curve shown in Fig. 8, relative humidity values in the range [5 %; 25 %] may be fit using the mathematical expression of the B.E.T model [32]:

$$\frac{HR}{(1-HR)W} = \frac{1}{CX_{12}} + \frac{C-1}{CX_{12}} HR \qquad (6)$$

where *HR* is relative humidity and *C* and X_{12} are constants. As shown in Fig. 8, fit quality is very good (R^2 in the range [0.84; 0.97]) for all test samples but alluvium sample #3 (R^2=0.66). Fit parameters *C* and X_{12} range in [-4.5; -1] and [-0.005; -0.249] respectively (note that these parameters would have positive values for actual water vapour adsorption isotherms, since parameter X_{12} for example denotes a water content). The transition point sought may be defined as the point where the fit significantly differs from actual curve, which may be identified graphically. For each curve depicted in Fig. 8, a blue arrow spots this transition point, whereas the intersection point of two perpendicular dotted lines highlights the achievement of the *SSD* state as determined from Table 3. Observe that the transition point provides a very good assessment of the *SSD* state, as confirmed by the last three rows of Table 3.

4. Conclusion and perspectives

An improved experimental setup was introduced in order to capture the *SSD* state of porous fine aggregates incorporating significant amounts of fines, such as recycled concrete fine aggregates. This setup was used to test three fine aggregate sources with different water absorption values up to 5.6 % (measured in the absence of fines) and at least 8 % of fines. Test duration was found to lie in the range 120-240 minutes, which suggests differences from the shorter duration reported by Kandhal et al [19]. Nevertheless, curves depicting water content shift as a function of drying time were found similar to those reported in the drying theory literature. As a consequence, the drying theory was used to fit these curves and a calculation procedure was explained in full detail to assess the *SSD* state. Fairly repeatable and discriminant water content values in *SSD* state were obtained using this procedure. As expected, these water absorption values were found significantly higher than those determined in the absence of fines according to the usual cone test [1]. Furthermore, the lack of reliability of water absorption values determined in the presence of fines according to the cone test procedure was verified. Besides, as reported by Dana et al and Kandhal et al [19,20], curves representing temperature gradient or relative humidity shift as a function of time were found to evidence drop breakpoints, however the latter appeared to be located closer to actual *SSD* state than the former. Eventually, a more straightforward strategy for assessing the water content in *SSD* state was suggested, which consists in identifying the transition point between retained and free water on charts representing the variations of water content as a function of relative humidity.

Although the experimental setup was found able to assess the water content of fine aggregates incorporating fines in *SSD* state - even in the case of recycled concrete fine aggregates thanks to moderate drying -, several perspectives should be pointed out. First, recorded curves tend to be noisy, which causes results scattering that could be avoided by using a more stable hot air generator setup. Second, test duration could be reduced upon optimizing the sample mass. Next, automation of the device would make no difficulty. Eventually, more theoretical work is needed to model the full outline of water content versus relative humidity curves determined using the experimental setup.

Acknowledgements

This paper was written in memory of Patrick Gentilini, who initiated this research.

The authors thank Florian Huchet, Maxime Piton, Lauredan Le Guen and Alexis Cothenet from IFSTTAR for helpful conversations.

5. References

[1] CEN. Tests for mechanical and physical properties of aggregates - Part 6: Determination of particle density and water absorption. 2014.

[2] Kasemchaisiri R, Tangtermsirikul S. A method to determine water retainability of porous fine aggregate for design and quality control of fresh concrete. Constr Build Mater 2007;21:1322–34. doi:10.1016/j.conbuildmat.2006.01.009.

[3] RILEM. RILEM recommendation I2I-DRG Guidance for demolition and reuse of concrete and masonry. Specifications for concrete with recycled aggregates. Mater Struct 1994;27:557–9.

[4] RILEM. STAR 217-PRE Progress of Recycling in the Built Environment (final draft). Springer, ISBN 978-94-007-4907-8. Available at http://www.springer.com/fr/book/9789400749078. 2013.

[5] De Larrard F. Concrete Mixture Proportioning: A Scientific Approach. 1999.

[6] Zhao Z, Remond S, Damidot D, Weiya X. Influence of fine recycled concrete aggregates on the properties of mortars. Constr Build Mater 2015;81:179–86.

[7] Khatib JM. Properties of concrete incorporating fine recycled aggregate. Cem Concr Res 2005;35:763–9. doi:10.1016/j.cemconres.2004.06.017.

[8] Evangelista L, de Brito J. Durability performance of concrete made with fine recycled concrete aggregates. Cem Concr Compos 2010;32:9–14. doi:10.1016/j.cemconcomp.2009.09.005.

[9] Kandhal PS, Lee DY. An Evaluation of the Bulk Specific Gravity for Granular Materials. Highw. Res. Board, Highw. Res. Rec., 1970, p. 44–55.

[10] Krugler PE, Tahmoressi M, Rand DA. Improving the Precision of Test Methods Used in VMA Determination. Asphal Paving Technol 1992;62:272–303.

[11] ASTM. C 128-07a: Standard Test Method for density, relative density (specific gravity) and absorption of fine aggregate. 2007.

[12] AASHTO. T84: Standard test method of test for specific gravity and absorption of fine aggregate. 2010.

[13] Lin P-J, Chuang Y-J. Determination of SSD condition of fine aggregates using AC impedance spectroscopy. Mater Struct 2013;46:911–20. doi:10.1617/s11527-012-9943-x.

[14] Saxer EL. A direct Method of Determining Absorption and Specific Gravity of Aggregates. Rock Prod 1956;87:77–9.

[15] You Z, Mills-Beale J, Williams RC and Dai Q. Measuring the Specific Gravities of Fine Aggregates: An Automated Procedure. Int J Pavement Res Technol 2009;2:37–50.

[16] DRE Bourgogne. Catalogue des matériaux de substitution en Bourgogne (in French). France: 2004.

[17] Gomes M, de Brito J, Bravo M. Mechanical Performance of Structural Concrete with the Incorporation of Coarse Recycled Concrete and Ceramic Aggregates. J Mater Civ Eng 2014;26:04014076. doi:10.1061/(ASCE)MT.1943-5533.0000973.

[18] Rogers C, Dziedziejko T. Fine aggregate density testing, what is the right way to do? 15th Annu. Symp. Res. - Int. Cent. Aggregates Res., 2007, p. A2–1 (24 p).

[19] Kandhal PS, Mallick RB, Huner M. Measuring Bulk Specific Gravity of Fine Aggregates: Development of a New Test Method. In: TRB, editor. Transp. Res. Rec. J. Transp. Res. Board, National Research Council; 2000, p. 81–90.

[20] Dana JS, Peters RJ. Experimental Moisture Determination for Defining Saturated Surface Dry State of Highway Aggregates (internal report). 1974.

[21] Mechling M, Lecomte A, Merriaux K. Mesure de l'absorption d'eau des additions minérales des bétons par vaporométrie (In French). Mater Struct 2003;36:32–9.

[22] Charreau A, Cavaillé R. Séchage. Théorie et calculs (In French) 1991:J 2 480–1 – 23.

[23] Tam VWY, Gao XF, Tam CM, Chan CH. New approach in measuring water absorption of recycled aggregates. Constr Build Mater 2008;22:364–9. doi:10.1016/j.conbuildmat.2006.08.009.

[24] Mindess S, Young F, Darwin D. Concrete. Prentice Hall; 2003.

[25] Poon CS, Chan D. Feasible use of recycled concrete aggregates and crushed clay brick as unbound road sub-base. Constr Build Mater 2006;20:578–85. doi:10.1016/j.conbuildmat.2005.01.045.

[26] CEN. Tests for geometrical properties of aggregates — Part 9: Assessment of fines - Methylene blue test. 2013.

[27] Khoury GA, Majorana ÃCE, Pesavento F, Schrefler BA. Modelling of heated concrete. Mag Concr Res 2002;54:77–101.

[28] Zhang Q, Ye G. Dehydration kinetics of Portland cement paste at high temperature. J Therm Anal Calorim 2012;110:153–8. doi:10.1007/s10973-012-2303-9.

[29] Gong F, Zhang D, Sicat E, Ueda T. Empirical Estimation of Pore Size Distribution in Cement , Mortar , and Concrete. J Mater Civ Eng 2014:1–11. doi:10.1061/(ASCE)MT.1943-5533.0000945.

[30] Sing KSW, Everett DH, Haul RAW, Moscou L, Pierotti RA, Rouquérol J, Siemieniewska T. INTERNATIONAL UNION OF PURE COMMISSION ON COLLOID AND SURFACE CHEMISTRY INCLUDING CATALYSIS * REPORTING PHYSISORPTION DATA FOR GAS / SOLID SYSTEMS with Special Reference to the Determination of Surface Area and Porosity. Pure Appl Chem 1985;57:603–19.

[31] Baroghel-Bouny V. Water vapour sorption experiments on hardened cementitious materials. Cem Concr Res 2007;37:414–37. doi:10.1016/j.cemconres.2006.11.019.

[32] Brunauer S, Emmett P, Teller E. Gases i n Multimolecular Layers. J Am Chem Soc 1938;60:309–19. doi:citeulike-article-id:4074706.